



Published in final edited form as:

Anal Chem. 2011 November 15; 83(22): 8366–8371. doi:10.1021/ac202016x.

DESI then MALDI mass spectrometry imaging of lipid and protein distributions in single tissue sections

Livia S Eberlin¹, Xioahui Liu², Christina R. Ferreira¹, Sandro Santagata³, Nathalie Y.R. Agar^{2,*}, and R. Graham Cooks^{1,*}

¹Department of Chemistry and Center for Analytical Instrumentation Development, Purdue University, West Lafayette, IN 47907 (USA)

²Department of Neurosurgery, Department of Radiology, and Department of Medical Oncology, Brigham and Women's Hospital and Dana-Farber Cancer Institute, Harvard Medical School, Boston, MA 02115 (USA)

³Department of Pathology, Brigham and Women's Hospital, Harvard Medical School, Boston, MA 02115(USA)

Abstract

Imaging mass spectrometry (MS) is a powerful technique for mapping the spatial distributions of a wide range of chemical compounds simultaneously from a tissue section. Co-localization of the distribution of individual molecular species including particular lipids and proteins, and correlation with the morphological features of a single tissue section is highly desirable for comprehensive tissue analysis and disease diagnosis. We now report on the use, in turn, of desorption electrospray ionization (DESI), matrix assisted laser desorption ionization (MALDI) and then optical microscopy to image lipid and protein distributions in a single tissue section. This is possible through the use of histologically compatible DESI solvent systems, which allow for sequential analyses of the same section by DESI then MALDI. Hematoxylin and Eosin (H&E) staining was performed on the same section after removal of the MALDI matrix. This workflow allowed chemical information to be unambiguously matched to histological features in mouse brain tissue sections. The lipid sulfatide(24:1), detected at m/z 888.8 by DESI imaging, was co-localized with the protein MBP isoform 8, detected at m/z 14117 by MALDI imaging, in regions corresponding to the corpus callosum substructure of the mouse brain, as confirmed in the H&E images. Correlation of lipid and protein distributions with histopathological features was also achieved for human brain cancer samples. Higher tumor cell density was observed in regions demonstrating higher relative abundances of oleic acid, detected by DESI imaging at m/z 281.4, and the protein calcyclin, detected by MALDI at m/z 10085, for a human glioma sample. Since correlation between molecular signatures and disease state can be achieved, we expect that this methodology will significantly enhance the value of MS imaging in molecular pathology for diagnosis.

Keywords

imaging mass spectrometry; desorption electrospray ionization; laser desorption; histology; tissue diagnosis

*Corresponding authors **Professor R. Graham Cooks**, Department of Chemistry, Purdue University, West Lafayette, IN, 47907, Tel: (+1) 765-494-5262, Fax: (+1) 765-494-9421, cooks@purdue.edu, **Dr. Nathalie Y. R. Agar**, Department of Neurosurgery, Brigham and Women's Hospital, Harvard Medical School, Boston, MA, 02115, Tel: (+1) 617-525-7374, Fax: (+1) 617-264-6316, nagar@bwh.harvard.edu.

Introduction

Imaging mass spectrometry, especially by MALDI¹, secondary ion mass spectrometry (SIMS)² and DESI³ has emerged as a powerful methodology for understanding biological systems. A wide range of analytes including drugs, drug metabolites, lipids, hormones, peptides, and proteins can be detected and imaged directly from tissue sections. MS imaging is particularly promising for disease diagnostics, notably recognition of neoplastic tissue⁴. In cancer research, most studies by imaging MS have used MALDI to map the distribution of proteins or peptides in tissue. More recently, however, differential lipid distributions or specific lipid species have been successfully correlated to diverse tumor types and grades using DESI^{3, 5}.

While MALDI is the most widespread high vacuum imaging technique in MS for peptide and protein analysis in tissues, it is also used for lipid analysis⁶. Recent applications of MALDI include imaging of glycerophospholipids in the ocular lens⁷ and imaging of bacterial colonies⁸. MALDI imaging utilizes a sample preparation step in which the tissue is homogeneously covered with an organic matrix for ionization⁹⁻¹⁰. The efficiency of ionization of different classes of molecules can be greatly influenced by the type of matrix that is used¹¹⁻¹². MALDI imaging of small molecules such as metabolites and drugs benefits from the use of low-background matrices (or no matrix at all) and the use of high mass resolution analyzers¹³⁻¹⁴.

Unlike MALDI and SIMS which are both performed in vacuum, a number of ambient ionization methods have been developed recently¹⁵. These approaches are based on direct examination of unprepared, unmodified samples in the open environment using a solvent spray, laser beam or plasma probe to affect both desorption of analytes from the sample and their ionization. DESI is a commonly used ambient MS technique for drug, metabolite and lipid imaging⁶. Emphasis in DESI applications has been on cancer diagnostics and grading, but it has also been used in other biological applications such as mapping changes in lipids associated with spinal cord trauma¹⁶, analyzing pigments and alkaloids in plant tissue¹⁷ and mapping cholesterol in brain using reactive DESI imaging¹⁸. Different solvents can be used in DESI imaging with the goal of increasing the ionization efficiency of certain molecules. Recently, significant progress has been achieved in analyzing tissue sections by DESI-MS imaging and in minimizing the destructive nature of the technique. In particular, the development of dimethylformamide (DMF)-based solvent combinations has enabled DESI-MS imaging to be performed with preservation of morphological features. As a result, histological and immunohistochemical analysis can be performed after the imaging experiment¹⁹. This enables DESI-MS imaging to be inserted at any point into a work flow for tissue analysis.

Assessing the lipid and protein profiles on the same section of tissue while preserving tissue morphology allows conventional histological examination and hence correlation between these three types of information. This can help advance MS-imaging as a practical diagnostic and research tool. This is especially useful in the analysis of tissue sections from tumors which can be highly heterogeneous, containing varied tumor cell concentrations²⁰, admixed normal and stromal tissues and dysplastic, pre-invasive lesions²¹, among other features. Obtaining lipid and protein information from the same tissue section could greatly increase the accuracy of molecular diagnoses and the understanding of the biochemical and pathophysiological processes underlying the malignant state. Most applications of MALDI-MS imaging utilize the spatial distributions of individual analytes of two compound classes, lipids and proteins. However, as experimental conditions used for lipid imaging are different from those used for proteins in terms of the matrix used, the mass/charge range and the acquisition mode (reflectron/linear) when using time-of-flight analyzers, only one

compound class is efficiently studied per tissue section using MALDI-MS imaging. At the same time, while DESI-MS imaging is a powerful and versatile ambient technique for lipid imaging with no need for matrix deposition, it has not yet been established for protein imaging in biological tissues. Therefore, non-identical serial sections are commonly used to acquire MS images and to assess histological features.²²

Here we demonstrate that a single tissue section initially used for DESI-MS imaging of lipids, can then be used for protein imaging by MALDI and then subsequently be stained with H&E to acquire morphological information. This approach combines the unique strengths of DESI and MALDI for lipid and protein imaging, respectively, and allows the unambiguous matching of morphological and chemical features (Figure 1), as we demonstrate for mouse brain and human brain cancer tissue samples.

Experimental section

Tissue samples

A frozen male mouse brain was stored at $-80\text{ }^{\circ}\text{C}$ until it was sliced into $10\text{ }\mu\text{m}$ thick sections using a Shandon SME Cryotome cryostat (GMI, Inc., Ramsey, MN, USA). Two tissue sections were thaw mounted onto conductive indium tin oxide (ITO) coated glass slides (BrukerDaltonics, Billerica, MA). One section was analyzed using DESI followed by MALDI and the control was only analyzed by MALDI. Four human brain cancer tissues were obtained from the Brigham Women's Hospital (BWH) Neurooncology Program Biorepository collection, and analyzed under approved Institutional Review Board (IRB) protocol, with informed written consent obtained by licensed neurosurgeons at BWH. The samples included two gliomas and two brain metastases. Human tissue samples were sectioned into $10\text{ }\mu\text{m}$ thick sections and thaw mounted onto ITO coated glass slides. Glass slides were stored at $-80\text{ }^{\circ}\text{C}$ until analysis, when they were allowed to come to room temperature and dried in a desiccator for ~ 15 minutes.

DESI for lipid imaging

The DESI imaging source used was a lab-built prototype²³, which was optimized for signal intensity and image quality²⁴. Two morphologically friendly solvent systems were used: ACN:DMF (1:1) and EtOH:DMF (1:1). Experiments were carried out in the negative ion mode, using a 5 kV spray voltage, a solvent flow rate of $0.7\text{ }\mu\text{L}/\text{min}$, and 175 psi of nebulizing gas (N_2) pressure. Mass spectra were acquired from m/z 200 to 1000. An incident angle of 54° to the surface plane was used for the DESI spray. The mass spectrometer used was a LTQ linear ion trap mass spectrometer controlled by XCalibur 2.0 software (Thermo Fisher Scientific, San Jose, CA, USA). The tissues were scanned using a 2D moving stage in horizontal rows separated by a vertical step of $150\mu\text{m}$ (mouse) or $200\mu\text{m}$ (human). An in-house program allowed the conversion of the XCalibur 2.0 mass spectra files (.raw) into a format compatible with Biomap (freeware, <http://www.maldi-msi.org>), on which spatially resolved images were assembled and displayed in the interpolated mode. The lipid species detected were tentatively identified based on collision-induced dissociation (CID) tandem MS experiments (Supporting Information) and comparison of the generated product ion spectra with literature data²⁴⁻²⁸. The fatty acids were tentatively assigned based on the mass of the molecular anion $[\text{M}-\text{H}]^{-}$. Isomers of lipids are known to occur, making these identifications tentative.

MALDI for protein imaging

After DESI imaging experiments, optical images of the slides were taken using a scanner (EPSON, CA) to direct tissue positioning in the TOF mass spectrometer. A matrix solution, $10\text{mg}/\text{mL}$ sinapinic acid (Sigma, St. Louis, MO) matrix was prepared. For mouse brain

tissues, the matrix was dissolved in 60% ACN, 40% H₂O with 0.2% TFA while for human brain samples, a fixative solution containing ethanol/methanol/acetonitrile/0.1% TFA (in water) in a ratio of 2:2:1:1 was used²². The matrix solution was homogeneously sprayed for ~90 minutes on each slide using ImagePrep (BrukerDaltonics, Germany). MALDI imaging was performed using a UltrafleXtreme MALDI-TOF/TOF (BrukerDaltonics, Germany) in the positive ion mode, using a 1 kHz smartbeam laser. Mass calibration was performed in the linear mode over the range from m/z 5734 to 16952. The MALDI imaging experiment was controlled by the program FlexImaging 3.0 (BrukerDaltonics, Germany). The laser diameter was set to ~50 μ m and rastered along the x- and y-axis of selected regions at 150 μ m or 200 μ m resolution. Each spectrum was acquired from 500 laser shots on a single spot operating the TOF MS in the linear mode. The mass/charge range over which ions were detected was m/z 600 to 20137. The MALDI images were analyzed with the software FlexImaging 3.0, and displayed using data interpolation.

Histochemistry

Tissue sections were subjected to H&E staining according to standard protocol (Supporting Information) after the MALDI matrix has been removed by washing using 70% ethanol (2 min) for mouse brain sections and 95% ethanol (1 min) for human tissues. The optical images of the tissues were obtained using the Axio Imager M1 microscope scanner system for telepathology (Zeiss, Chester, VA) at 40X magnification. Digital images of the human tissue samples were used for detailed neuropathological evaluation using the Mirax Digital Slide Desktop server application (Zeiss, Chester, VA).

Results and Discussion

Mouse brain

Lipid imaging by DESI-MS—Characteristic lipid profiles were observed when DESI-MS imaging was performed on mouse brain tissue sections using two morphologically friendly solvent systems, ACN:DMF (1:1) and EtOH:DMF (1:1). Very little interference due to background ions from the solvent system and from the glass slides was observed across the full m/z range, resulting in high spectral intensity and good contrast in the ion images. Two distinctive MS peak patterns were observed in the negative ion mode for the mouse brain sections, which are associated with the white and gray matter regions of the brain tissue as previously reported using DESI imaging with conventional solvent systems, such as MeOH:H₂O (1:1)^{23–24}. In the low m/z range (m/z 200 – m/z 400) the majority of the ions observed are due to free fatty acids while the majority of the ions observed in the high m/z range (m/z 700 – m/z 1000) correspond to lipids such as phosphatidylserines (PS), phosphatidylinositols (PI) and sulfatides (ST). Two-dimensional ion images of specific lipids are shown in Figure 2, using ACN:DMF (1:1) as solvent system. Distinctive and complementary spatial distributions were observed for ions m/z 283.5, FA(18:0) (A) and m/z 834.6 (PS(18:0/22:6)) (B), observed at higher abundance in the brain gray matter, and m/z 888.8, ST(h24:1) (C), observed in the brain white matter. Tandem MS spectra are shown for m/z 834.6 and m/z 888.8 in Figures S1 and S2, Supporting Information, respectively.^{25, 28} An averaged DESI mass spectrum of the tissue section is shown in Figure 3A and this includes spectra from regions of white and gray matter.

Protein Imaging by MALDI-MS—The same mouse brain tissue section previously analyzed by DESI using ACN:DMF was prepared with sinapinic acid matrix and then analyzed using MALDI-MS under the same raster resolution settings. The most abundant proteins observed were in the mass range 4000 Da–15000 Da (Figure 3B). All protein assignments are tentative and based on previous reports.^{29–31} Representative protein images are shown in Figure 2D–F. While both PEP-19 (6718Da, Figure 2D) and neurogranin

(7532Da, Figure 2E) are located in the gray matter, neurogranin is more abundant in the cortex region with expression in both superficial and deep cortical layers. PEP-19 is also present in the cortex but is present predominantly in the deeper layers of the cortex and also in the thalamus^{29,31}. Myelin basic protein (MBP) isoform 8 is found predominantly in the white matter of mouse brain (Figure 2F)³⁰. This experiment demonstrates that DESI-MS can be used to extract lipid species while conserving the protein content and at least some features of its distribution in the tissue section.

Co-localization of lipid and proteins by DESI/MALDI in mouse brain—Does prior DESI-MS imaging alter the quality of the data obtained by MALDI-MS and the distribution of proteins? To access this information, we performed MALDI imaging on a control serial tissue section that was mounted adjacent to the section imaged by DESI, on the same ITO glass slide. Comparison between the ion intensities of the proteins detected in the control section and one previously analyzed by DESI-MS (Figure 3B and 3C, respectively) revealed very similar total and relative intensities of proteins detected. Very similar results were obtained whether the tissue sections were imaged using EtOH:DMF (1:1) or ACN:DMF (1:1) solvents. Most importantly, prior DESI-MS imaging of lipids using either solvent system did not disturb the native protein localization. This finding is consistent with results obtained by immunostaining of tissues that were subjected to DESI-MS imaging with similar solvents¹⁹. Proteins with distinctive preferential distributions within white and gray matter were observed at their expected locations even after DESI imaging had been performed. Ion images of control tissue sections showed very similar protein spatial distributions. Co-localization of lipids and proteins was observed for many of the species detected. For example, the lipid species detected at m/z 888.8 by DESI-MS imaging, assigned as ST(24:1), is in its majority co-localized with the protein species at m/z 14117, assigned as MBP isoform 8, detected by MALDI-MS imaging. Both of these species are mostly localized within the brain's white matter, in substructures such as the corpus callosum, and their distribution further correlates with the expression of MBP detected by mRNA in situ hybridization reported in the Allen Brain Atlas (<http://mouse.brain-map.org/welcome.do>) (Figure S3, Supporting Information). In another example, PS(18:0/22:6) (m/z 834.6) and neurogranin (m/z 7531) are detected by DESI-MS and MALDI-MS imaging with fairly similar distributions in the gray matter, with both having higher relative intensities in the cerebral cortex substructure and coinciding with the mRNA expression of neurogranin (Figure S3, Supporting Information). However, a general limitation of imaging mass spectrometry is the occurrence of matrix effects, and this means that it is not possible to be sure that the observed lipids and proteins accurately and completely represent the tissue constituents.

The ability to perform histological analysis of tissue sections after subsequent DESI and MALDI MS imaging was evaluated next. Figure 2G–I show optical images of the H&E stained tissue after DESI and MALDI analyses. Substructures of the mouse brain can be observed in the images of regions 1 (Figure 2H) and 2 (Figure 2I), such as the corpus callosum (white matter) observed in region 2. These images showcase the preservation of tissue morphology even after two MS imaging analysis events. Optical images of the H&E stained tissue sections that were either first imaged by DESI-MS using EtOH:DMF (1:1) and then imaged by MALDI-MS, and of a control tissue section which was only imaged by MALDI are shown in Figure S4 (Supporting Information). While some tissue cracking and sliding occurred in both tissue sections, morphological information is conserved with this methodology, allowing chemical and histological information to be matched.

DESI and MALDI imaging of lipids and proteins in human glioma

Assessment of the spatial distribution of lipids and proteins in a single tissue section provides the opportunity for more complete chemical understanding of tumor tissue composition. Unambiguous correlation of the biochemical information obtained by MS imaging with the diagnostic information provided by pathology is important for accurately assigning biomarker signatures to disease states. Figure 4 shows the results obtained for a sample of human glioma grade III, which was first imaged by DESI, followed by MALDI imaging, and then optical imaging after H&E staining. Comprehensive lipid information was obtained by DESI-MS imaging of the tissue section (Figure 4D), allowing detection of many fatty acids and different glycerolipids, such as m/z 885.5, PI(18:0/20:4); m/z 747.5, PG(16:0/18:1) and m/z 281.4, FA(18:1), oleic acid. Tandem MS spectra are shown for m/z 885.5 and m/z 747.5 in Figures S5 and S6, Supporting Information, respectively.^{26–27} The low abundance of sulfatide species observed is in agreement with reported DESI imaging data for higher grade astrocytomas³². Protein imaging by MALDI was performed on the same tissue section after DESI imaging. Within the many protein peaks detected (Figure 4H), fatty acid-binding protein 5, m/z 15064, and calcyclin, m/z 10085, have been reported to be expressed in human gliomas, allowing discrimination of gliomas from normal brain tissue³³. Interestingly, correlation between the spatial distribution of lipids and proteins within the tissue section was observed for many species. For example, the distribution of the phospholipids PI(18:0/20:4), m/z 885.5 (Figure 4A), and PG(16:0/18:1), m/z 747.5 (Figure 4B), was similar to the distribution of the fatty acid-binding protein 5, m/z 15064 (Figure 4E), while a similar distribution of oleic acid, m/z 281.4 (Figure 4C), and calcyclin, m/z 10085 (Figure 4F), was observed in the respective ion images. H&E staining of the same tissue section revealed sufficient preservation of morphological criteria to allow appropriate diagnostic evaluation of the tumor (Figure 4G). While the distribution of glioma cells was relatively homogenous in this sample, slightly higher tumor cell density was observed by histopathological evaluation in regions demonstrating relatively high abundances of oleic acid and calcyclin. In addition, necrotic regions co-localized with regions that showed a higher intensity of PI(18:0/20:4), PG(16:0/18:1) and fatty acid-binding protein 5. Analysis of a control tissue section which had not been subjected to DESI-MS imaging revealed very similar spatial distributions of the proteins selected (Figure 4I–J). The distribution of the proteins also correlated to areas of higher tumor cell density, as observed by evaluation of H&E stained section (Figure 4K). Similar protein distribution was also observed in the mass spectra of the control tissue section (Figure 4L). Slight variations in distribution and ion intensity could be associated to differences in morphological features between the different tissue sections, as observed in the other human brain samples analyzed.

Conclusions

In this work, we show that lipid and protein images can be acquired by sequential DESI and MALDI imaging of the same tissue section. Since tissue morphology is preserved after both analyses, the sample can be stained by H&E after solvent removal of the organic matrix used for MALDI. We applied both MS imaging techniques in the analysis of single tissue sections of mouse brain and human tumor samples followed by evaluation of the histology by a neuropathologist using bright-field microscopy. This workflow allows chemical information of two classes of molecules to be unambiguously matched to histological features. This is the first time that the DESI and MALDI methodologies have been used together to increase the chemical information obtained from a single tissue section. This study introduces a new methodology that has the potential to be used for the routine applications of MS imaging technology.

The speed and versatility of DESI-MS imaging makes it suitable for lipid analysis under ambient conditions. MALDI-MS imaging, then allows the detection of proteins and

peptides. Coupling imaging of lipids by DESI-MS and protein imaging by MALDI-MS enables a more complete evaluation of a single tissue section sample and provides high density chemical information for biomarker discovery. Ideally imaging both lipids and proteins could be performed in one experiment using a single methodology that preserves tissue morphology. Both the imaging MS techniques, however, still have limitations that makes the present hybrid methodology a good approach for same-tissue-section lipid and protein MS imaging. By mapping lipid and protein species from the same tissue section which is subsequently H&E stained, we expect to enhance diagnostic capabilities and allow insights into the pathophysiology of disease.

Supplementary Material

Refer to Web version on PubMed Central for supplementary material.

Acknowledgments

LSE thanks the ACS Division of Analytical Chemistry and Agilent Technologies for research summer fellowship. LSE, CRF and RGC thank the U.S. National Institute of Health (Grant 1R21EB009459-01) and the Purdue University Center for Cancer Research and its director Dr. Timothy Ratliff for assistance and support. NYRA thanks the DFCI Low-Grade Astrocytoma (PLGA) Program, the BWH Institute for the Neurosciences and the NIH Director's New Innovator Award (Grant 1DP2OD007383-01). SSA acknowledges the support of the National Institutes of Health (K08NS064168) and the V Foundation for Cancer Research. LSE gratefully acknowledges Prof. Demian R. Ifa of York University for valuable discussions.

References

1. Seeley EH, Schwamborn K, Caprioli RM. *J. Biol. Chem.* 2011; 286:25459–25466. [PubMed: 21632549]
2. Passarelli MK, Winograd N. *Biochim. Biophys. Acta.* 2011 in press.
3. Eberlin LS, Ferreira CR, Dill AL, Ifa DR, Cooks RG. *Biochim. Biophys. Acta Mol. Cell Biol. Lipids.* 2011 in press.
4. Vickerman JC. *Analyst.* 2011; 136:2199–2217. [PubMed: 21461433]
5. Dill AL, Eberlin LS, Ifa DR, Cooks RG. *Chem. Commun.* 2011; 47:2741–2746.
6. Watrous JD, Alexandrov T, Dorrestein PC. *J. Mass Spectrom.* 2011; 46:209–222. [PubMed: 21322093]
7. Pol J, Vidova V, Hyotylainen T, Volny M, Novak P, Strohalm M, Kostianen R, Havlicek V, Wiedmer SK, Holopainen JM. *PLoS One.* 2011; 6:e19441. [PubMed: 21559377]
8. Yang YL, Xu Y, Kersten RD, Liu WT, Meehan MJ, Moore BS, Bandeira N, Dorrestein PC. *Angew. Chem.-Int. Ed.* 2011; 50:5839–5842.
9. Schwamborn K, Caprioli RM. *Mol. Oncol.* 2010; 4:529–538. [PubMed: 20965799]
10. Ferguson L, Bradshaw R, Wolstenholme R, Clench M, Francese S. *Anal. Chem.* 2011; 83:5585–5591. [PubMed: 21667965]
11. Fuchs B, Suss R, Schiller J. *Prog. Lipid Res.* 2011; 49:450–475. [PubMed: 20643161]
12. McCombie G, Knochenmuss R. *Anal. Chem.* 2004; 76:4990–4997. [PubMed: 15373433]
13. Miura D, Fujimura Y, Yamato M, Hyodo F, Utsumi H, Tachibana H, Wariishi H. *Anal. Chem.* 2010; 82:9789–9796. [PubMed: 21043438]
14. Goodwin RJ, Pitt AR, Harrison D, Weidt SK, Langridge-Smith PR, Barrett MP, Logan Mackay C. *Rapid Commun. Mass Spectrom.* 2011; 25:969–972. [PubMed: 21416534]
15. Harris GA, Galhena AS, Fernandez FM. *Anal. Chem.* 2011; 83:4508–4538. [PubMed: 21495690]
16. Girod M, Shi Y, Cheng JX, Cooks RG. *Anal. Chem.* 2011; 83:207–215. [PubMed: 21142140]
17. Muller T, Oradu S, Ifa DR, Cooks RG, Krautler B. *Anal. Chem.* 2011; 83:5754–5761. [PubMed: 21675752]
18. Wu C, Ifa DR, Manicke NE, Cooks RG. *Anal. Chem.* 2009; 81:7618–7624. [PubMed: 19746995]

19. Eberlin LS, Ferreira CR, Dill AL, Ifa DR, Cheng L, Cooks RG. *ChemBioChem*. 2011; 12:2129–2132. [PubMed: 21793152]
20. Agar NYR, Golby AJ, Ligon KL, Norton I, Mohan V, Wiseman JM, Tannenbaum A, Jolesz FA. *Neurosurgery*. 2011; 68:280–290. [PubMed: 21135749]
21. Eberlin LS, Dill AL, Costa AB, Ifa DR, Cheng L, Masterson T, Koch M, Ratliff TL, Cooks RG. *Anal. Chem*. 2010; 82:3430–3434. [PubMed: 20373810]
22. Agar NY, Yang HW, Carroll RS, Black PM, Agar JN. *Anal. Chem*. 2007; 79:7416–7423. [PubMed: 17822313]
23. Wiseman JM, Ifa DR, Song QY, Cooks RG. *Angew. Chem.-Int. Ed*. 2006; 45:7188–7192.
24. Eberlin LS, Ifa DR, Wu C, Cooks RG. *Angew. Chem. Int. Edit*. 2010; 49:873–876.
25. Gao F, Tian XK, Wen DW, Liao J, Wang T, Liu HW. *Biochim. Biophys. Acta Mol. Cell Biol. Lipids*. 2006; 1761:667–676.
26. Hsu FF, Turk J. *J. Am. Soc. Mass Spectrom*. 2000; 11:986–999. [PubMed: 11073262]
27. Hsu FF, Turk J. *J. Am. Soc. Mass Spectrom*. 2001; 12:1036–1043.
28. Pulfer M, Murphy RC. *Mass Spectrom. Rev*. 2003; 22:332–364. [PubMed: 12949918]
29. Burnum KE, Frappier SL, Caprioli RM. *AnnU. Rev. Anal. Chem*. 2008; 1:689–705.
30. Crecelius AC, Cornett DS, Caprioli RM, Williams B, Dawant BM, Bodenheimer B. *J. Am. Soc. Mass Spectrom*. 2005; 16:1093–1099. [PubMed: 15923124]
31. Skold K, Svensson M, Nilsson A, Zhang XQ, Nydahl K, Caprioli RM, Svenningsson P, Andren PE. *J. Proteome Res*. 2006; 5:262–269. [PubMed: 16457591]
32. Eberlin LS, Dill AL, Golby AJ, Ligon KL, Wiseman JM, Cooks RG, Agar NYR. *Angew. Chem.-Int. Ed*. 2010; 49:5953–5956.
33. Schwartz SA, Weil RJ, Thompson RC, Shyr Y, Moore JH, Toms SA, Johnson MD, Caprioli RM. *Cancer Res*. 2005; 65:7674–7681. [PubMed: 16140934]

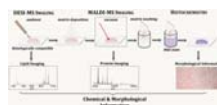


Figure 1. Schematic of the workflow used to perform DESI-MS and MALDI-MS imaging on the same tissue section thaw mounted onto an ITO glass slide, followed by H&E staining.

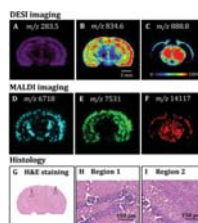


Figure 2.

DESI-MS ion images of a mouse brain coronal section (Bregma ~ -2.800 mm) using a histologically compatible solvent ACN:DMF (1:1) and showing the distribution of **(A)** m/z 283.5, FA(18:0), stearic acid; **(B)** m/z 834.3, PS(18:0/22:6) and **(C)** m/z 888.6, ST(24:1). After DESI-MS imaging, the same tissue section was subjected to MALDI-MS imaging. Ion images are shown for ions **(D)** m/z 6718, PEP19; **(E)** m/z 7531, neurogranin and **(F)** m/z 14117, MBP isoform 8. Optical image of the same tissue section after removal of the MALDI matrix and H&E staining is shown in **(G)**. High magnification views of different morphological regions are shown in **(H)** and **(I)**.

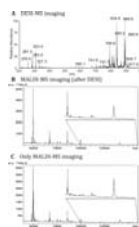


Figure 3.

(A) Averaged negative ion mode DESI-MS mass spectrum over the range m/z 200 – 1000 of a mouse brain tissue section, including regions of white and gray matter. (B) MALDI-MS averaged mass spectrum from m/z 4000 to m/z 15000 for the same tissue section. (C) Averaged mass spectrum of a control section which was imaged solely by MALDI-MS.

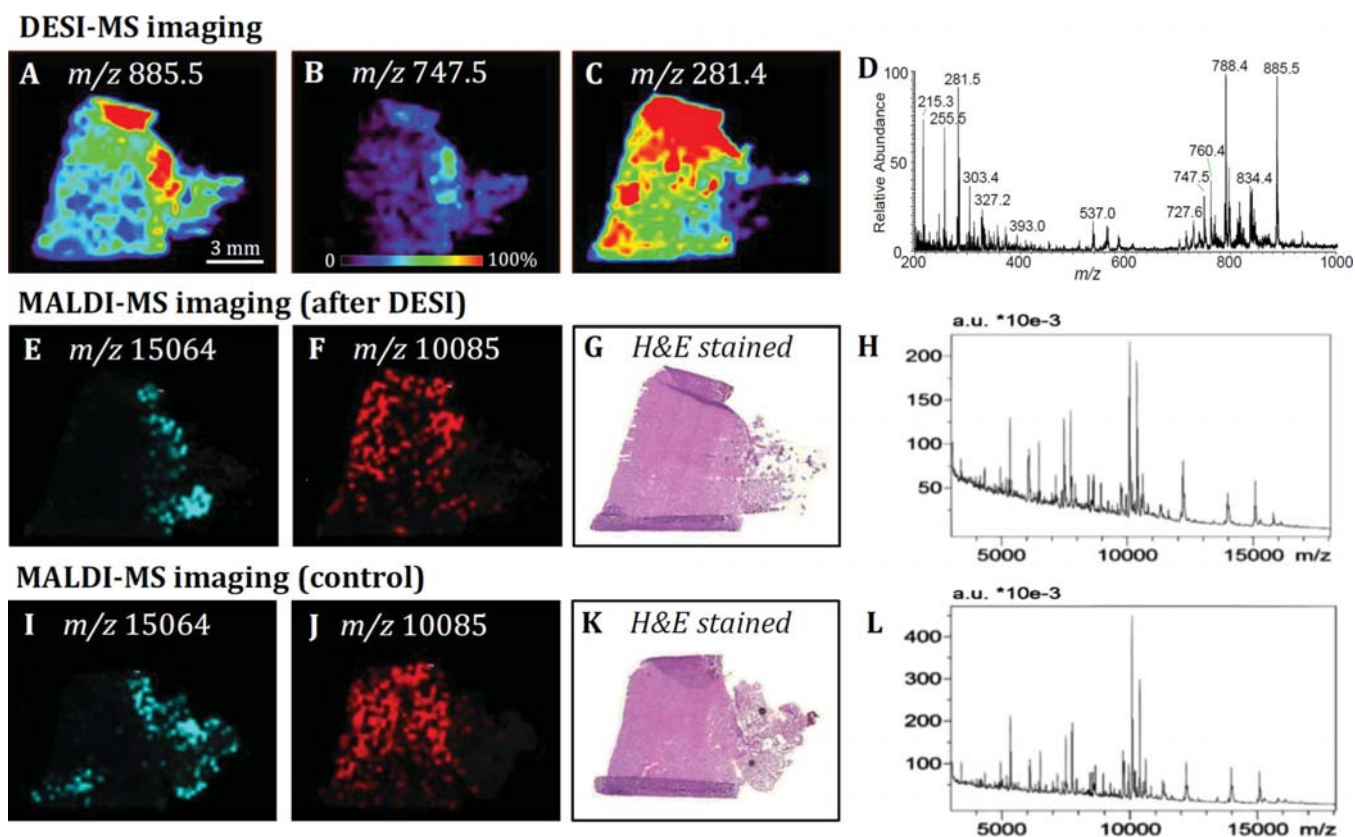


Figure 4. DESI-MS ion images of a human glioma samples using a histologically compatible solvent ACN:DMF (1:1), showing the distribution of **(A)** m/z 885.5, PI(18:0/20:4); **(B)** m/z 747.5, PG(16:0/18:1) and **(C)** m/z 281.4, FA(18:1), oleic acid. **(D)** Averaged negative ion mode DESI-MS mass spectra. After DESI-MS imaging, the same tissue section was subjected to MALDI-MS imaging. Ion images are shown for ions **(E)** m/z 15064, fatty acid-binding protein 5, and **(F)** m/z 10085, calcyclin. **(G)** Optical image of the same tissue section after H&E staining. **(H)** MALDI-MS average positive ion mode mass spectra of the same tissue section. Ion images of control tissue section are shown for same ions **(I)** m/z 15064, fatty acid-binding protein 5, and **(J)** m/z 10085, calcyclin. **(K)** Optical image of the same tissue section after H&E staining. **(L)** MALDI-MS averaged positive ion mode mass spectra of the control tissue section.